of *HI* compared to reoptimization, although the amplitude was small. The change in *CI* was not statistically significant for any imaging dose.

Effects of reoptimization on OAR dose

Figure 3A illustrates changes in the rectal D_{mean} value from nonimaging values. While both compensation and reoptimization plans showed an imaging dose-dependent increase in rectal D_{mean}, reoptimization significantly suppressed dose elevation by half compared with compensation ($p < 0.001$ for all MU). Whereas the D_{mean} value of compensation plans became larger than observed with portal imaging when 8- to 15-MU CBCT was added, the D_{mean} value of reoptimization plans did not exceed that of portal imaging. Figure 3B shows the changes in gEUD from nonimaging plans. For the simple addition of portal imaging and 3-MU CBCT, the amplitude of gEUD elevation was similar to that of D_{mean}. In contrast, gEUD determined by both techniques changed modestly with every imaging dose. Because gEUD reflects the effect of inhomogeneous dose distribution, the cause of the disagreement seen in these results may be found in the dose-volume analysis (Fig. 3C). The rectal *Vx* value was uniformly elevated by addition of portal imaging and 3-MU CBCT. In contrast, compensation plans showed a remarkable increase of low-dose volume (V30–V50), while the changes in high-dose volume (V60–V70) were modest. The *Vx* elevations, especially those of low-dose volumes, were suppressed by reoptimization. No significant difference was noted between V60 for compensation and reoptimization plans when 3-MU CBCT was added, and there was no significant difference in V70 for all MU.

Figure 4 shows results for bladder doses subjected to the same analyses as those conducted above. The bladder D_{mean} value was also increased with increasing imaging dose (Fig. 4A). Unlike the results for the rectum, however, gEUD increased significantly for compensation and reoptimization plans compared with nonimaging values (Fig. 4B), and reoptimization significantly suppressed the gEUD elevation when 5 to 15 MU were added ($p = 0.008$ and 0.001 and $p < 0.001$ for 5 and 8 and 15 MU, respectively). As the analysis of *Vx* (Fig. 4C) shows, V70 was increased with increasing CBCT dose, and reoptimization significantly suppressed V70 elevation when 5 to 15 MU

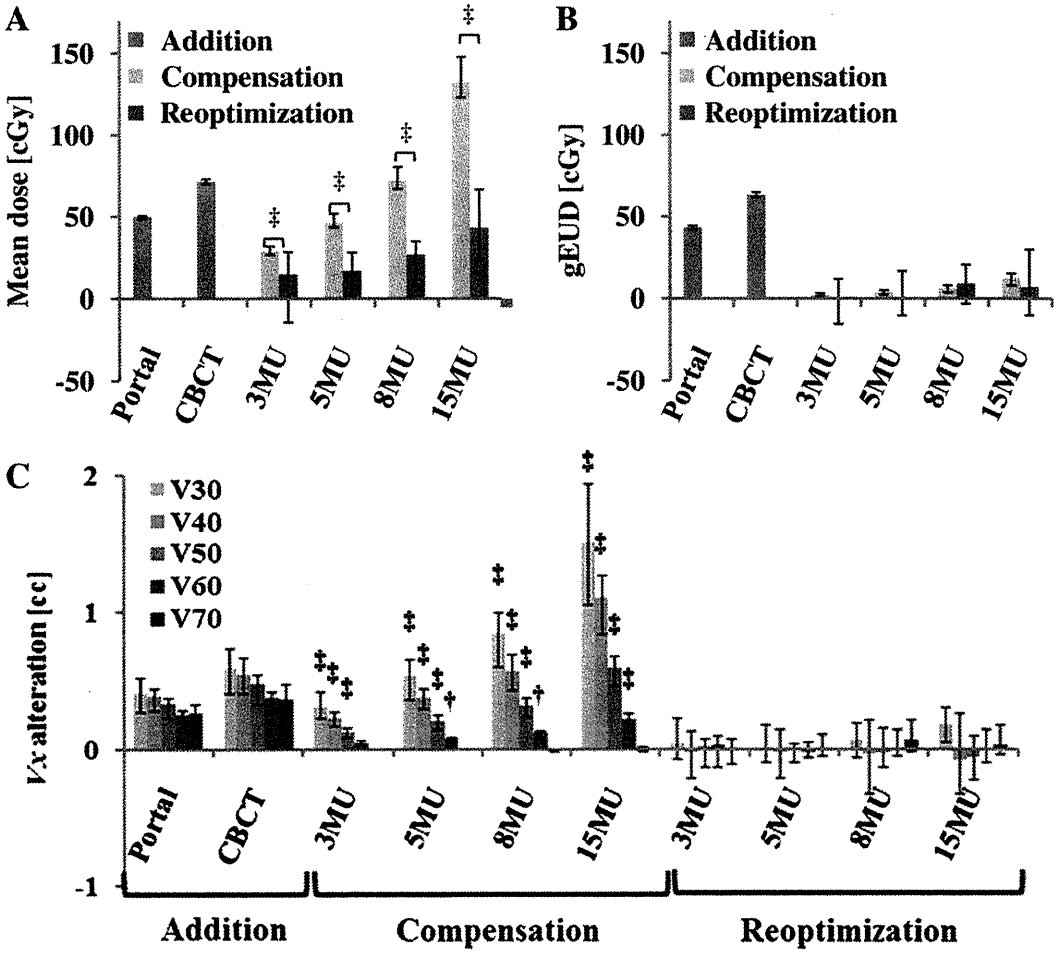

Fig. 3. The effects of MV-CBCT integration on rectal dose. The D_{mean} (A), gEUD (B), and *Vx* (C) values are shown. Each value represents the change from those of nonimaging plans. Columns and bars represent median and interquartile range, respectively. †, $p < 0.05$; ‡, $p < 0.01$. (Paired *t*-test comparisons between compensation and reoptimization plans with the same MU are shown).

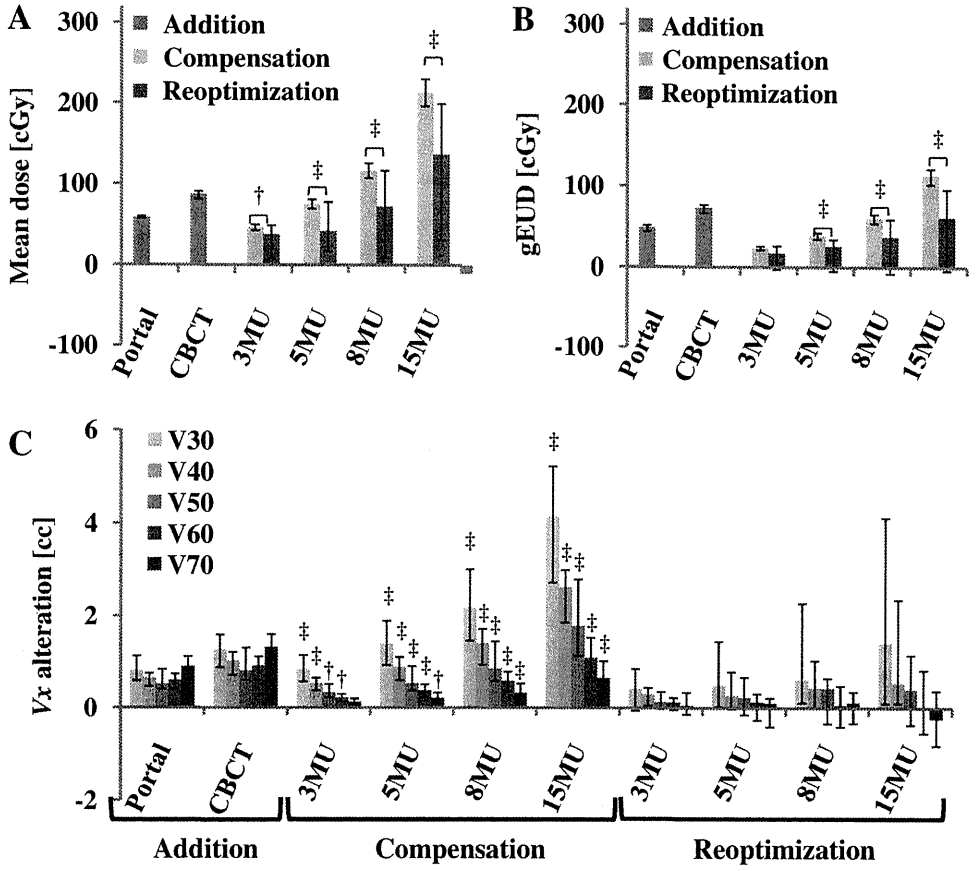

Fig. 4. The effects of MV-CBCT integration on bladder dose are shown. The D_{mean} (A), gEUD (B), and *Vx* (C) values are shown. Each value represents the change from those of nonimaging plans. Columns and bars represent median and interquartile range, respectively. †, $p < 0.05$; ‡, $p < 0.01$. (Paired *t*-test comparisons between compensation and reoptimization plans with the same MU are shown).

were added ($p = 0.044$ and 0.009 and $p < 0.001$ for 5 MU and 15 MU, respectively).

DISCUSSION

The accurate calculation of MV-CBCT dose distribution is essential to the integration of imaging dose with prescribed dose. Here, we were able to accurately calculate MV-CBCT dose distribution by using our method, even for quite low MU (Fig. 1B–D). We confirmed the fact that this method also allowed the accurate calculation of dose in differently shaped phantoms and that the stability of the MV-CBCT beam output was ensured by weekly measurement, routinely performed for IMRT quality assurance. We conclude that our method is feasible for any imaging dose, if the stability of beam output is confirmed by scheduled measurements. Similarly, the report of the American Association of Physicists in Medicine Task Group 142 recommended annual or more frequent assessment of imaging dose (25).

Regarding target coverage, compensation plans showed slightly decreased *HI* (Fig. 2C), indicating a decrease in hot or cold regions in the target volume. This is attributed to the uniform dose distribution of the MV-CBCT dose. However, the alteration was quite small and might be considered clinically negligible. Because the results of *HI* and *CI* demonstrated that MV-CBCT dose integration with both techniques did not worsen the quality of target coverage, the necessity of reoptimization can be simply evaluated by considering the effects of imaging dose on critical organs.

For the rectal D_{mean} value, reoptimization seemed to have a significant advantage for suppressing rectal dose elevation upon addition of imaging dose, particularly for high-MU CBCT (Fig. 3A). However, gEUD values for both techniques showed negligible changes from nonimaging values (Fig. 3B). The results of dose-volume analysis (Fig. 3C) explain the cause of the disagreement: compensation plans mainly increased low-dose volume (30–50 Gy), while their alteration of high-dose volume was modest. In contrast, simple addition of both portal imaging and 3-MU CBCT uniformly increased rectal *Vx*. In general, rectal complications result from high doses (26). Although many studies have demonstrated the association of late rectal toxicity with high dose (≥60 Gy), rectal bleeding correlates with the volume exposed to intermediate doses (40–60 Gy) (26, 27). Jackson et al. (27) stated that the intermediate dose might be associated with the recovery of tissue exposed to high dose. While compensation might be sufficient for reducing rectal injury, reoptimization could still be beneficial for reducing the volume receiving intermediate dose.

Although MV-CBCT dose increased both rectal and bladder D_{mean} values, the amplitude of the bladder dose elevation was larger than that of the rectal dose (Figs. 3A and 4A). The dose distribution of MV-CBCT is arch-shaped, indicating that the anterior region receives a relatively higher dose than the isocenter (Fig. 1A). Interestingly, the bladder but not rectal gEUD value increased with imaging dose. As Figure 4C shows, a significant increase in bladder V60 to V70 was observed in compensation plans. This increase can also be explained by the arch-shaped dose distribution of MV-CBCT. When PTV D95 is normalized to the prescribed dose by scaling down IMRT beams, insufficient compensation will result in the increased bladder dose, even for high *Vx*. Reoptimization significantly reduced bladder gEUD by modifying beam intensity and reduced high-dose volume (V60–V70) when 5 to 15 MU were added. Although little information about dose-volume relationship related to genitourinary toxicity was provided, Zelefsky et al. (28) reported a 20% incidence in late Grade ≥2 toxicity after 81-Gy prostate IMRT compared to a 12% incidence for non-IMRT patients treated with lower doses. While conformal RT techniques enable dose escalation, the bladder receives a localized but higher dose than with conventional RT. In patients in whom frequent MV-CBCT acquisition with high MU elevates the dose to this organ, reoptimization will be beneficial in reducing the risk of complications.

CONCLUSIONS

Many institutions may use MV-CBCT less frequently (*i.e.*, once weekly) or with low MU (*i.e.*, 3–5 MU) because of increased dose to normal tissue. For institutions using portal imaging for daily setup, portal imaging can be replaced by 3-MU CBCT because its dose is low and close to that of portal imaging. However, dose compensation is still valuable for reducing OAR dose. In that case, the low-MU CBCT calculation method described here would facilitate dose compensation. As our present study shows, compensation is sufficient for reducing the OAR dose increased by low-MU CBCT, and reoptimization is unnecessary. In contrast, for high-MU CBCT, reoptimization is obviously beneficial for reducing OAR dose, especially for the bladder. Appropriate application of these measures should allow accurate treatment with smaller PTV margins that result in fewer complications.

REFERENCES

1. Morin O, Gillis A, Chen J, *et al.* Megavoltage cone-beam CT: System description and clinical applications. *Med Dosim* 2006; 31:51–61.
2. Gayou O, Parda DS, Johnson M, *et al.* Patient dose and image quality from mega-voltage cone-beam computed tomography imaging. *Med Phys* 2007;34:499–506.
3. Gayou O, Miften M. Commissioning and clinical implementation of a mega-voltage cone beam CT system for treatment localization. *Med Phys* 2007;34:3183–3192.
4. Bylund KC, Bayouth JE, Smith MC, *et al.* Analysis of interfraction prostate motion using megavoltage cone beam computed tomography. *Int J Radiat Oncol Biol Phys* 2008;72: 949–956.
5. Aubry JF, Cheung J, Morin O, *et al.* Correction of megavoltage cone-beam CT images of the pelvic region based on phantom measurements for dose calculation purposes. *J Appl Clin Med Phys* 2009;10:33–42.
6. Petit SF, van Elmpt WJ, Lambin P, *et al.* Dose recalculation in megavoltage cone-beam CT for treatment evaluation: removal of cupping and truncation artifacts in scans of the thorax and abdomen. *Radiother Oncol* 2010;94:359–366.
7. Peng LC, Yang CC, Sim S, *et al.* Dose comparison of megavoltage cone-beam and orthogonal-pair portal images. *J Appl Clin Med Phys* 2007;8:10–20.
8. Stützel J, Oelfke U, Nill S. A quantitative image quality comparison of four different image guided radiotherapy devices. *Radiother Oncol* 2008;86:20–24.
9. Faddegon BA, Wu V, Pouliot J, *et al.* Low dose megavoltage cone beam computed tomography with an unflattened 4 MV beam from a carbon target. *Med Phys* 2008;35:5777–5786.
10. Flynn RT, Hartmann J, Bani-Hashemi A, *et al.* Dosimetric characterization and application of an imaging beam line with a carbon electron target for megavoltage cone beam computed tomography. *Med Phys* 2009;36:2181–2192.
11. Ezzell GA, Galvin JM, Low D, *et al.* Guidance document on delivery, treatment planning, and clinical implementation of IMRT: Report of the IMRT subcommittee of the AAPM radiation therapy committee. *Med Phys* 2003;30:2089–2115.
12. Galvin JM, Ezzell G, Eisbrauch A, *et al.* Implementating IMRT in clinical practice: A joint document of the American Society for Therapeutic Radiology and Oncology and the American Association of Physicists in Medicine. *Int J Radiat Oncol Biol Phys* 2004;58:1616–1634.
13. Antolak JA, Rosen II, Childress CH, *et al.* Prostate target volume variations during a course of radiotherapy. *Int J Radiat Oncol Biol Phys* 1998;42:661–672.
14. Zellars RC, Roberson PL, Strawderman M, *et al.* Prostate position late in the course of external beam therapy: Patterns and predictors. *Int J Radiat Oncol Biol Phys* 2000;47:655–660.
15. de Crevoisier R, Melancon AD, Kuban DA, *et al.* Changes in the pelvic anatomy after an IMRT treatment fraction of prostate cancer. *Int J Radiat Oncol Biol Phys* 2007;68:1529–1536.
16. Adamson J, Wu Q. Inferences about prostate intrafraction motion from pre- and posttreatment volumetric imaging. *Int J Radiat Oncol Biol Phys* 2009;75:260–267.
17. van Haaren PM, Bel A, Hofman P, *et al.* Influence of daily setup measurements and corrections on the estimated delivered dose during IMRT treatment of prostate cancer patients. *Radiother Oncol* 2009;90:291–298.
18. Morin O, Gillis A, Descovich M, *et al.* Patient dose considerations for routine megavoltage cone-beam CT imaging. *Med Phys* 2007;34:1819–1827.
19. Miften M, Gayou O, Reitz B, *et al.* IMRT planning and delivery incorporating daily dose from mega-voltage cone-beam computed tomography imaging. *Med Phys* 2007;34:3760–3767.
20. Morin O, Aubry JF, Aubin M, *et al.* Physical performance and image optimization of megavoltage cone-beam CT. *Med Phys* 2009;36:1421–1432.
21. Seuntjens J, Olivares M, Evans M, *et al.* Absorbed dose to water reference dosimetry using solid phantoms in the context of absorbed-dose protocols. *Med Phys* 2005;32:2945–2953.

22. Low DA, Harms WB, Mutic S, *et al.* A technique for the quantitative evaluation of dose distributions. *Med Phys* 1998;25: 656–661.
23. Niemierko A. A generalized concept of equivalent uniform dose (EUD). *Med Phys* 1999;26:1100 (Abstract).
24. Burman C, Kutcher GJ, Emami B, *et al.* Fitting of normal tissue tolerance data to an analytic function. *Int J Radiat Oncol Biol Phys* 1991;21:123–135.
25. Klein EE, Hanley J, Bayouth J, *et al.* Task Group 142 report: Quality assurance of medical accelerators. *Med Phys* 2009; 36:4197–4212.
26. Michalski JM, Hiram Gay, Jackson A, *et al.* Radiation dose-volume effects in radiation-induced rectal injury. *Int J Radiat Oncol Biol Phys* 2010;76:S123–S129.
27. Jackson A, Skwarchuk MW, Zelefsky MJ, *et al.* Late rectal bleeding after conformal radiotherapy of prostate cancer. II. Volume effects and dose-volume histograms. *Int J Radiat Oncol Biol Phys* 2001;49:685–698.
28. Zelefsky MJ, Levin EJ, Hunt M, *et al.* Incidence of late rectal and urinary toxicities after three-dimensional conformal radiotherapy and intensity-modulated radiotherapy for localized prostate cancer. *Int J Radiat Oncol Biol Phys* 2008;70:1124–1129.

JJCO Japanese Journal of Clinical Oncology

Jpn J Clin Oncol 2011;41(5)609–616
doi:10.1093/jjco/hyr022
Advance Access Publication 16 March 2011

Significance of Tumor Volume Related to Peritumoral Edema in Intracranial Meningioma Treated with Extreme Hypofractionated Stereotactic Radiation Therapy in Three to Five Fractions

Masahiro Morimoto[1,*], Yasuo Yoshioka[1], Hiroya Shiomi[1], Fumiaki Isohashi[1], Koji Konishi[1], Tadayuki Kotsuma[1], Shoichi Fukuda[1], Naoki Kagawa[2], Manabu Kinoshita[2], Naoya Hashimoto[2], Toshiki Yoshimine[2] and Masahiko Koizumi[3]

[1]Department of Radiation Oncology, Osaka University Graduate School of Medicine, [2]Department of Neurosurgery, Osaka University Graduate School of Medicine and [3]Division of Medical Physics, Oncology Center, Osaka University Hospital, Suita, Osaka, Japan

*For reprints and all correspondence: Masahiro Morimoto, 2-2 Yamadaoka, Suita, Osaka 565-0871, Japan. E-mail: morimoto-knk@umin.ac.jp

Received December 23, 2010; accepted January 31, 2011

Background: To investigate the treatment results of intracranial meningiomas treated with hypofractionated stereotactic radiation therapy in three to five fractions.
Methods: Thirty-one patients (32 lesions) with intracranial meningioma were treated with hypofractionated stereotactic radiation therapy in three to five fractions using CyberKnife. Fifteen lesions were diagnosed as Grade I (World Health Organization classification) by surgical resection and 17 lesions were diagnosed as meningioma based on radiological findings. The median follow-up time was 48 months. The median planning target volume was 6.3 cm^3 (range, 1.4–27.1), and the prescribed dose (D90≤) ranged from 21 to 36 Gy (median, 27.8) administrated in three to five fractions.
Results: Five-year overall and progression-free survival rate of all 31 patients with intracranial meningioma was 86 and 83%, respectively. Five-year progression-free rate of all 32 lesions was 87%. Six of the 31 patients (19%) developed marked peritumoral edema, three of whom were asymptomatic and three symptomatic, the latter with late adverse effects of more than or equal to Grade 3. The mean planning target volume of the six lesions with marked peritumoral edema was 15.6 cm^3, and for the remaining 26 lesions without marked peritumoral edema was 7.1 cm^3 ($P = 0.004$). The threshold diameter of 2.56 cm for meningioma was calculated from the planning target volume (11 cm^3) and was used as marker of developing peritumoral edema ($P = 0.003$).
Conclusions: Tumor volume is a significant indicative factor for peritumoral edema in intracranial meningioma treated with hypofractionated stereotactic radiation therapy in three to five factions.

Key words: intracranial meningioma – stereotactic radiation therapy – CyberKnife – peritumoral edema – tumor volume

INTRODUCTION

Surgical resection is the main treatment for intracranial meningioma (1). However, radiation therapy may also be considered for a tumor which is not suitable for resection, a residual or recurrent tumor after surgical resection, and the presence of factors, which contraindicate surgical resection such as low performance status, advanced age or complications. For such cases, conventional radiation therapy remains the preferred modality (2–5), but stereotactic radiation therapy has recently come into worldwide use (6–12). According to previous reports, results for stereotactic

[†]Presented in part at the 69th annual meeting of the Japan Radiological Society (2010) in Yokohama, Japan.

radiation therapy for intracranial meningioma were comparable to those for conventional radiation therapy, but severe adverse effects, such as peritumoral edema of intracranial meningioma, have been also reported. The risk factors of the peritumoral edema of intracranial meningioma are mainly reported in radiosurgery (13–28). However, there have been few reports on the risk factors of the peritumoral edema of intracranial meningioma treated with hypofractionated stereotactic radiation therapy in three to five fractions.

The purpose of this study was to investigate the treatment results for intracranial meningiomas treated with hypofractionated stereotactic radiation therapy in three to five fractions using CyberKnife and the risk factors for peritumoral edema as an adverse effect.

PATIENTS AND METHODS

Between June 1999 and June 2008, 31 patients (32 lesions) with intracranial meningioma were treated with extreme hypofractionated stereotactic radiation therapy in three to five fractions using CyberKnife at Osaka University Hospital, Japan. Eligibility criteria for this treatment were: (i) patients with tumors which were not suitable for resection; (ii) patients with residual or recurrent tumors after surgical resection; (iii) patients with factors contraindicative of surgical resection such as low performance status, severe complications or advanced age; (iv) patients with symptoms caused by the tumor. In principle, the criterion for size was a meningioma of <3 cm. Patient characteristics and treatment parameters are listed in Table 1. The median age was 68 years old (range, 18–90), and there were 27 female and 4 male patients. One patient (two lesions) was diagnosed with neurofibromatosis type II. Fifteen lesions were diagnosed as Grade I (World Health Organization classification) by surgical resection or biopsy and the remaining 17 lesions as meningioma based on radiological findings or clinical course. The types and locations of the 32 meningiomas were parasagittal meningiomas (8), falx (5), petroclival (4), cavernous sinus, convexity (3 each), sphenoidal ridge, tentorial, cerebellopontine angle (2 each), and clival, middle cranial fossa, anterior clinoidal (1 each). The median follow-up time was 48 months (range, 10–127) and the median radiological follow-up time was 40 months (range, 1–125).

The CyberKnife (Accuray, Sunnyvale, CA, USA) is a stereotactic radiation therapy system with a 6-MV X-band linac on a robot arm controlled along six axes. The guidance system uses X-ray radiographic imaging to track the treatment site and control the alignment of radiation beams from the robot-mounted liniac. Shiomi et al. (29) reported that the accuracy of this system as used at our hospital was 0.7 mm (median). A thermoplastic plastic shell is used for fixation of the patient. At our hospital, enhanced computed tomography (CT) with a 1.25 mm slice thickness was performed with the patient in the treatment position. The gross tumor volume (GTV) was defined as the visible lesion detected by enhanced CT with reference to magnetic resonance imaging (MRI). The clinical target volume (CTV) was defined as being of the same size as the GTV. The planning target volume (PTV) was defined in principle as expansion of 0.1 cm of the CTV in all directions, with a median PTV of 6.3 cm^3 (range, 1.4–27.1). For 14 of 32 lesions, we chose the treatment plan in which at least 90% of the PTV was included within the prescribed isodose line (D90$\leq$). The remaining 18 were treated with a prescribed dose of D90, which represents the dose with which 90% of the tumor volume is irradiated. Our prescribed dose ranged from 21 to 36 Gy (median, 27.8) in three to five fractions. Twenty-one gray in three fractions was used for 2 of the patients, 24 Gy in three fractions for 12 patients (13 lesions), 25.5 Gy in three fractions for 1 patient, 30 Gy in three fractions for 11 patients, 30 Gy in four fractions for 1 patient, 30 Gy in five fractions for 3 patients and 36 Gy in three fractions for 1 patient. The total dose and fractionation for each patient were decided at weekly meetings of the radiation oncologists and the neuro-oncologists. However, the actual dose often changed the dose according to the distance to the risk organs or other patient factors, and it often depended on the judgment of the primary doctor.

The dose was converted to the biologically equivalent dose (BED) normalized to 2 Gy in 1 fraction (NTD of 2 Gy) based on the following linear quadratic equation [BED =

Table 1. Patient characteristics and treatment parameters

Patients	31 (32 lesions)
Male	4
Female	27
Diagnosed pathologically	15
Diagnosed with radiological findings	17
The median age (range)	68 (18–90)
The median follow-up time (range)	48 months (10–127)
Tumor location	
Parasagittal	8
Falx	5
Petroclival	4
Cavenous sinus	3
Convexity	3
Sphenoidal ridge	2
Tentorial	2
Cerebellopontine angle	2
Clival	1
Middle cranial fossa	1
Anterior clinoidal	1
The median total dose (90 $\leq$ D) (range)	27.8 Gy (21–36)
The median fractionation (range)	3 (3–5)
The median planning target volume (range)	6.3 cm^3 (1.4–27.1)

number of fractions × dose per fraction × (1 + dose per fraction/(α/β)], $\alpha/\beta = 10$ for early responding tissue, $\alpha/\beta = 3$ for late responding tissue). NTD 2 Gy, $\alpha/\beta = 10$ of stereotactic radiation therapy ranged from 29.8 to 66 Gy (median, 39.7), and its NTD 2 Gy, $\alpha/\beta = 3$ counterpart from 42 to 108 Gy (median, 54). Stereotactic radiation therapy was delivered at one fraction a day which took about 1.5 to 1 h to complete. All three to five fractions were administrated on consecutive days except in case of holidays.

Our patients were routinely followed up every 0.5–12 months and follow-up MRI was performed routinely. The tumor diameter in the *X*, *Y* and *Z* planes on MRI was determined for every case and the tumor size was classified as decreased, increased or unchanged. A decrease in tumor size was defined as one of the three diameters of the tumor as observed on MRI having decreased after treatment to less than half of what it was before the treatment. An increase in tumor size was defined as one of the three diameters having increased after treatment to more than 1.5 times of what it was before the treatment. Unchanged tumor size was defined as not meeting for either a decrease or an increase. This classification is a modified version of the one by Selch et al. (30). The patients with tumors unchanged or decreased in size were defined as progression free.

Late adverse effects were defined as symptoms that occurred more than 3 months after stereotactic radiation therapy. Common terminology criteria for adverse events, v4.0 were adopted for evaluation of such effects (31). Edema was defined as marked peritumoral edema if it developed >3 cm from the edge of the tumor as observed on T2-weighted MRI after stereotactic radiation therapy.

Retrospective treatment results were analyzed for evaluation of the following clinical endpoints: overall survival rate, progression-free survival rate, progression-free rate, the appearance rate of marked peritumoral edema and the frequency of adverse events more than or equal to Grade 3. Overall survival rate, progression-free survival rate and progression-free rate were measured from the beginning of stereotactic radiation therapy of the meningioma and were estimated with the Kaplan–Meier method. Significant differences between groups were tested with *t*-test or Fishers exact test. The findings of multivariate analysis were tested with sequence regression analysis. The *P* value was two-sided, and a *P* value of 0.05 or less was considered significant. SPSS, version 12.0 (SPSS, Inc., Chicago, IL, USA) was used for all statistical analyses.

RESULTS

Overall Survival, Progression-Free Survival and Progression-Free Rates

Five-year overall and progression-free survival rate of all 31 patients with intracranial meningioma were 86% (Fig. 1A) and 83% (Fig. 1B), respectively. Five-year progression-free rate for all 32 lesions was 87% (Fig. 1C). One patient (2 lesions) who was diagnosed with neurofibromatosis type II was alive with lesions unchanged at last the follow-up. Of the 32 lesions, 3 were judged to have decreased, 25 to have remained unchanged and 4 to have increased, with the latter estimated to have increased at 25, 29, 37 and 105 months, respectively, after stereotactic radiation therapy. The respective PTV and treatment doses were 3.3 cm^3 (24 Gy in three fractions), 9.6 cm^3 (30 Gy in three fractions), 24.1 cm^3 (30 Gy in three fractions) and 27.1 cm^3 (30 Gy in three fractions) and their locations were parasagittal (2), clival and falx (1 each). Three patients underwent salvage treatment, two patients surgical resection, one patient re-stereotactic radiation therapy. Three patients with increased meningiomas died of the disease at 30, 43 and 68 months after the initial treatment. In addition to these three, three others died for a total of 6 deaths. These other three patients whose meningioma was controlled died of lung cancer, diabetes mellitus and gastrointestinal bleeding, respectively.

Marked Peritumoral Edema and Adverse Events

Six of the 31 patients (19%) developed marked peritumoral edema, 3 asymptomatic and 3 symptomatic with late adverse effects more than or equal to Grade 3. Three of the symptomatic patients developed seizure, gait disturbance and central nervous system necrosis accompanied by loss due to long-term heightened intracranial pressure. One of the three patients whose PTV of convexity meningioma was 14.2 cm^3 developed seizure (Grade 3) 3 months after treatment with 24 Gy in three fractions and often required hospitalization to control the seizure. One of the three patients whose PTV of falx meningioma was 22.2 cm^3 developed gait disturbance (Grade 3) 5 months after treatment with 30 Gy in five fractions. This patent was confined to a wheelchair and died of gastrointestinal bleeding from unknown causes 8 months after the initial stereotactic radiation therapy. The last of the three patients whose PTV of cavernous sinus meningioma was 13.1 cm^3 developed central nervous system necrosis (Grade 4) 9 months after treatment with 36 Gy in three fractions (Fig. 2A). She developed bilateral vision loss associated with bilateral papilledemas and marked peritumoral edema (Fig. 2B,C) and underwent a craniotomy to reduce the intracranial pressure. The necrotic tissue around the tumor was confirmed pathologically. After 8 years, the marked peritumoral edema seen in Fig. 2C was comparatively resolved (Fig. 2D). She was alive with bilateral vision loss at the last follow-up. The respective PTV, treatment dose and location of the marked peritumoral edema in the 3 asymptomatic patients were 5.9 cm^3 (24 Gy in three fractions, falx), 11.4 cm^3 (30 Gy in four fractions, sphenoidal ridge) and 27.1 cm^3 (30 Gy in three fractions, parasagittal).

A scatter chart of the PTVs with or without marked peritumoral edema is shown in Fig. 3. We performed univariate analysis. The mean PTV of the 6 lesions with peritumoral

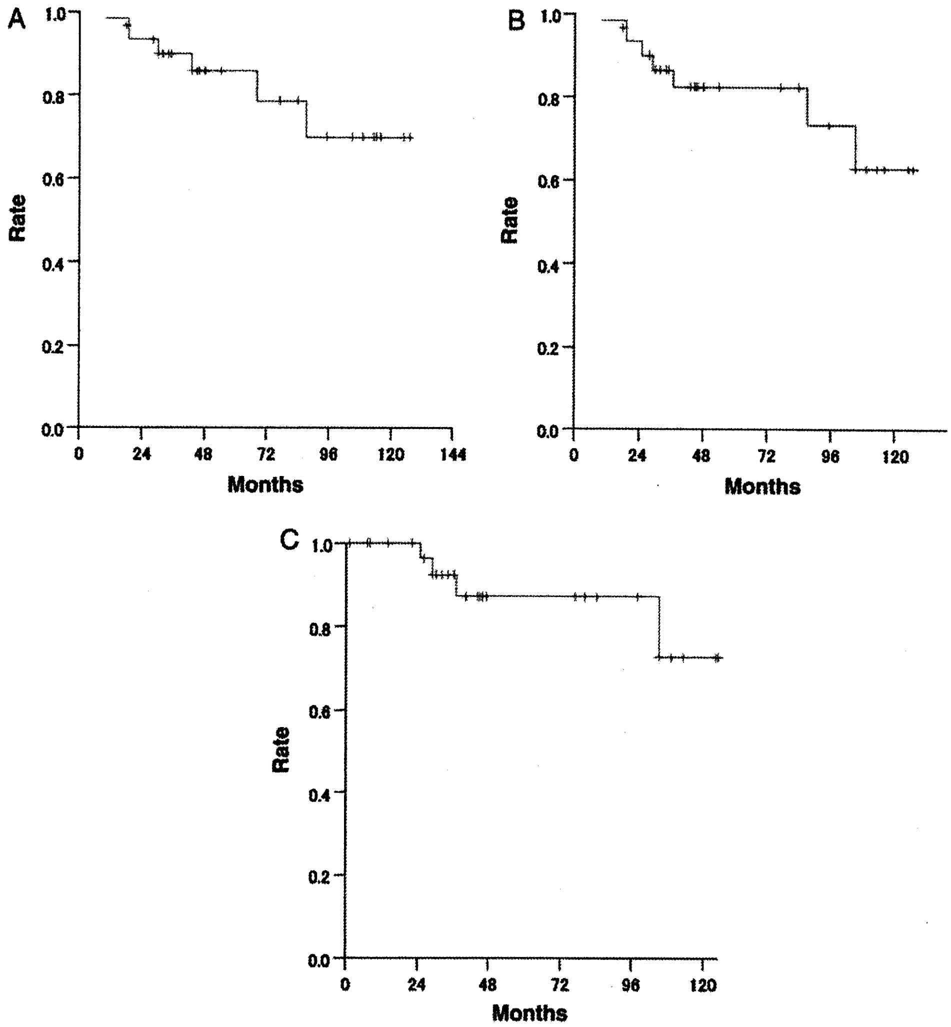

Figure 1. (A) Overall survival rate of meningioma patients ($n = 31$). (B) Progression-free survival rate of meningioma patients ($n = 31$). (C) Progression-free rate of meningioma lesions ($n = 32$).

edema was 15.6 cm^3, whereas that of the 26 lesions without marked peritumoral edema was 7.1 cm^3 ($P = 0.004$). We determined the threshold of the PTV with the strongest correlation with marked peritumoral edema and found that PTV of 11 cm^3 correlated most strongly ($P = 0.003$). We further assumed that the tumor was a spherical and adopted the following formula for calculation: PTV (cm^3) $= 4/3 \times \pi \times$ (GTV diameter (cm)/2 + 0.1 cm)^3. For a PTV of 11 cm^3, the diameter of the GTV was 2.56 cm. Of the 32 lesions, 9 GTV diameters were >2.56 cm and 5 of the 9 diameters were associated with marked peritumoral edema. Of the 32 lesions, 23 diameters of the GTV were $\leq$2.56 cm and 1 of the 23 diameters were associated with marked peritumoral edema. Intracranial meningiomas with a GTV diameter of more than 2.56 cm developed significantly marked peritumoral edema.

The total dose and schedule with or without peritumoral edema was converted to NTD of 2 Gy, $\alpha/\beta = 3$, and the respective average total doses were 68.1 and 62.0 Gy. The difference in dosage between tumors with and without peritumoral edema was not significant ($P = 0.377$). The most frequent sites of the tumors with peritumoral edema was falx, but this location turned out not to be significant factor in peritumoral edema ($P = 0.102$). We also performed multivariate analysis of PTVs dose and location. The results showed that PTVs was a marginally significant factor ($P = 0.066$), while the dose ($P = 0.372$) and the location ($P = 0.493$) were not.

DISCUSSION

Clinical endpoints in this study were comparable to those of other published study reports (2–12).

Reports on treatment of peritumoral edema with stereotactic radiosurgery have appeared in the literature since the 1990s. Engenhart et al. (13) reported that 5 of 17 meningioma patients (29%) developed a large area of brain edema resulting from treatment with single high-dose radiation therapy using a linac accelerator. Since then, the frequency

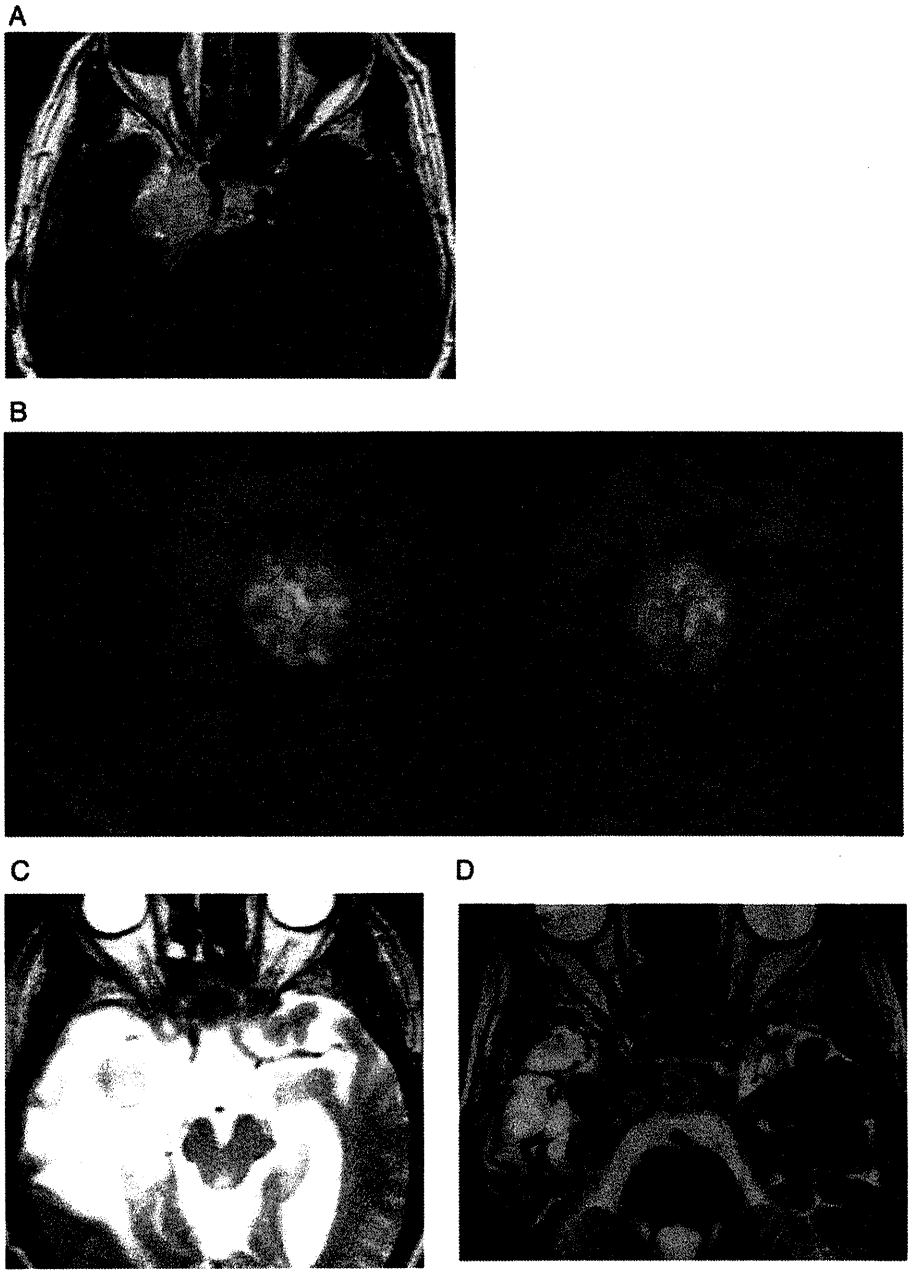

Figure 2. (A) Enhanced T1-weighted magnetic resonance image before stereotactic radiation therapy. The well-defined enhanced tumor which was compatible with meningioma is indicated in the right cavenous sinus. (B) Bilateral eye-fundus images 9 months after stereotactic radiation therapy. Bilateral papilledemas are indicated and were due to intracranial high pressure. (C) T2-weighted magnetic resonance image after stereotactic radiation therapy of 9 months. Marked peritumoral edema was indicated. (D) T2-weighted magnetic resonance image 8 years after stereotactic radiation therapy. Marked peritumoral edema was resolved compared with the image in (C).

and the risk factors of peritumoral edema have been widely discussed. The frequency of mainly radiosurgery-induced edema has been reported as 6–43% (13–28). The risk factors of peritumoral edema resulting from treatment with stereotactic radiation therapy are summarized in Table 2 (20–28). Patil et al. (20) reported that the risk factor was parasagittal location, mainly for stereotactic radiosurgery using CyberKnife. Chang et al. (21) reported that location or dose was the risk factors of peritumoral edema with Gamma Knife. Ganz et al. (22) reported that patients treated with Gamma Knife developed edema preferentially in case of non-basal tumors, especially those around the midline and sagittal sinus. In all but one case where radiation-induced edema was observed was the margin tumor dose 18 Gy or more. Kalapurakal et al. (23) reported that the risk factors of peritumoral edema were parasagittal location, presence of pretreatment edema, sagittal sinus occulusion, use of >6 Gy per fraction for liniac stereotactic radiosurgery and radiation therapy. Cai et al. (24) stated that the risk factors of peritumoral edema were tumor–brain contact interface area and

tumor volume for meningioma treated with Gamma Knife. Kollova et al. (25) found that the risk factors were age >60 years, no previous surgery, presence of pretreatment edema, tumor volume >10 cm^3, tumor location in anterior fossa and marginal dose >16 Gy for treatment with Gamma Knife. Novotny et al. (26) reported that no previous surgery, edema present before stereotactic radiosurgery, tumor volume >10 cm^3, location in anterior fossa and maximum dose >30 Gy were risk factors for peritumoral edema with Gamma Knife. The importance of the tumor location was thus most often reported in radiosurgery, whereas the importance of the tumor volume was reported only in Gamma Knife. Kan et al. (27) reported that molecular factors for

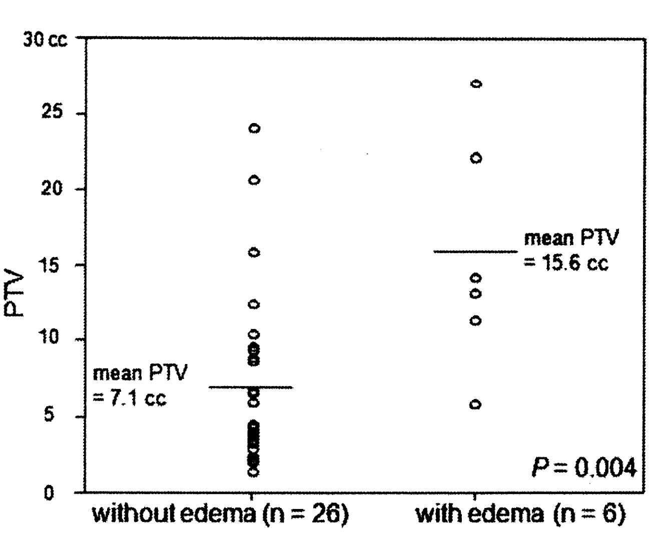

Figure 3. Scatter chart of the planning target volume (PTV) with or without marked peritumoral edema ($n = 32$). The difference in mean PTV was significant ($P = 0.004$)

peritumoral edema included vascular endothelial growth factor of peritumoral edema after stereotactic radiosurgery for intracranial meningiomas. Chen et al. (32) described the causes of peritumoral edema as radiation necrosis, infiltration of inflammatory cells and radiation injury to the vasculature causing hyalinization of blood vessels. On the other hand, Selch et al. reported no treatment-induced peritumoral edema resulting from fractionated stereotactic radiation therapy with 50.4 Gy in 28 fractions (30). Finally, Girvigian et al. reported that fractionated stereotactic radiation therapy (median, 50.4 Gy in 28 fractions) was associated with less risk of post-treatment symptomatic peritumoral edema compared with stereotactic radiosurgery treatment with a marginal dose of 14 Gy (28).

Most of the reports on the risk factors of peritumoral edema in association with meningioma are concerned with radiosurgery, while there have been hardly any reports of the risk factors of tumor volume for peritumoral edema resulting from hypofractionated stereotactic radiation therapy with three to five fractions. In our study, marked peritumoral edema was observed in 6 of 31 patients (19%), a rate which was not high compared with other reports. As for the biological aspects, extreme hypofractionation was found to be more harmful to normal cerebral tissue than conventional radiation therapy because the α/β level of cerebral tissue is supposed to be low. However, indication of meningioma with the small volume (the PTV $\leq$11 cm^3, diameter $\leq$2.56 cm) for hypofractionated stereotactic radiation therapy has made it possible to reduce severe adverse effects. Our study offers suggestions as to which meningiomas can be indicated for stereotactic radiation therapy with three to five fractions. We could not determine in our study whether tumor location is a significant factor. The number of patients might not be enough to reveal the difference in the incidence

Table 2. The significant risk factors of the peritumoral edema in patients treated with stereotactic radiation therapy

Investigator	Modality	Case	Total dose (Gy)	Fractions	Risk factors
Chang et al. (21)	GK	140	15	1	Tumor location, dose
Ganz et al. (22)	GK	35	12	1	Tumor location, dose
Kollova et al. (25)	GK	331	12.5	1	Tumor location, tumor volume, age, no previous surgery, presence of pretreatment edema
Novotny et al. (26)	GK	331	12.5	1	Tumor location, tumor volume, dose, no previous surgery, presence of pretreatment edema
Cai et al. (24)	GK	182	13.6	1	Tumor–brain contact interface, tumor volume, presence of pretreatment edema
Kalapurakal et al. (23)	Linac	43	13.5–54	≤1	Tumor location, dose, sagittal sinus occulusion, presence of pretreatment edema
Kan et al. (27)	Linac	18	13–15	1	Molecular marker
Girvigian et al. (28)	Linac	32	14 or 50.4	1 or 28	Single fraction
Patil et al. (20)	CK	102	18	1	Tumor location
Present study	CK	31	27.8	3	Tumor volume

GK, Gamma Knife; CK, CyberKnife.

of peritumoral edema among the locations of the tumor. We guessed another possibility that unlike treatment with a single fraction, three to five fractions could overcome the problem of the location compared with a single fraction. Hashiba et al. (33) reported that the proliferative potential of meningioma can be predicted from radiologic characteristics and 16 of 70 incidentally discovered meningiomas were found to have been grown exponentially (34). The treatment timing of stereotactic radiation therapy for such meningiomas with rapid growth should therefore be considered carefully.

In conclusion, tumor volume was identified as a significant factor for peritumoral edema in intracranial meningioma treated with extreme hypofractionated stereotactic radiation therapy in three to five factions using CyberKnife. Specifically, careful attention should be paid when treating meningiomas >2.56 cm in diameter. We have not been able to establish a unified treatment or patient criteria in stereotactic radiation therapy for meningioma at our institution. We therefore had to establish our treatment strategy for meningiomas based on the analyses performed in this study. From now on, we will deliver 24 Gy in three fractions for meningioma in principle and be more careful not to treat large meningiomas with the PTVs >11 cm^3 or close to the risk organs in the regimen. We will consider more fractionations for these cases according to need.

Acknowledgements

We deeply appreciated the following investigators who contributed to this study: Iori Sumida, PhD, Yutaka Takahashi, PhD and Toshiyuki Ogata, MS (Division of Medical Physics, Oncology Center, Osaka University Hospital).

Conflict of interest statement

None declared.

References

1. Alexiou GA, Gogou P, Markoula S, Kyritsis AP. Management of meningiomas. *Clin Neurol Neurosurg* 2010;112:177–82.
2. Goldsmith BJ, Wara WM, Wilson CB, Larson DA. Postoperative irradiation for subtotally resected meningiomas. A retrospective analysis of 140 patients treated from 1967 to 1990. *J Neurosurg* 1994;80:195–201.
3. Nutting C, Brada M, Brazil L, Sibtain A, Saran F, Westbury C, et al. Radiotherapy in the treatment of benign meningioma of the skull base. *J Neurosurg* 1999;90:823–7.
4. Maire JP, Caudry M, Guerin J, Celerier D, San Galli F, Causse N, et al. Fractionated radiation therapy in the treatment of intracranial meningiomas: local control, functional efficacy, and tolerance in 91 patients. *Int J Radiat Oncol Biol Phys* 1995;33:315–21.
5. Kokubo M, Shibamoto Y, Takahashi JA, Sasai K, Oya N, Hashimoto N, et al. Efficacy of conventional radiotherapy for recurrent meningioma. *J Neurooncol* 2000;48:51–5.
6. Onodera S, Aoyama H, Katoh N, Taguchi H, Yasuda K, Yoshida D, et al. Long-term outcomes of fractionated stereotactic radiotherapy for intracranial skull base benign meningiomas in single institution. *Jpn J Clin Oncol* (Epub), 22 December 2010.
7. Villavicencio AT, Black PM, Shrieve DC, Fallon MP, Alexander E, Loeffler JS. Linac radiosurgery for skull base meningiomas. *Acta Neurochir (Wien)* 2001;143:1141–52.
8. Stafford SL, Pollock BE, Foote RL, Link MJ, Gorman DA, Schomberg PJ, et al. Meningioma radiosurgery: tumor control, outcomes, and complications among 190 consecutive patients. *Neurosurgery* 2001;49:1029–37.
9. Pollock BE. Stereotactic radiosurgery for intracranial meningiomas: indications and results. *Neurosurg Focus* 2003;14:e4.
10. Kondziolka D, Madhok R, Lunsford LD, Mathieu D, Martin JJ, Niranjan A, et al. Stereotactic radiosurgery for convexity meningiomas. *J Neurosurg* 2009;111:458–63.
11. Takanashi M, Fukuoka S, Hojyo A, Sasaki T, Nakagawara J, Nakamura H. Gamma knife radiosurgery for skull-base meningiomas. *Prog Neurol Surg* 2009;22:96–111.
12. Colombo F, Casentini L, Cavedon C, Scalchi P, Cora S, Francescon P. Cyberknife radiosurgery for benign meningiomas: short-term results in 199 patients. *Neurosurgery* 2009;64:A7–13.
13. Engenhart R, Kimmig BN, Hover KH, Wowra B, Sturm V, van Kaick G, et al. Stereotactic single high dose radiation therapy of benign intracranial meningiomas. *Int J Radiat Oncol Biol Phys* 1990;19:1021–6.
14. Nakamura S, Hiyama H, Arai K, Nakaya K, Sato H, Hayashi M, et al. Gamma knife radiosurgery for meningiomas: four cases of radiation-induced edema. *Stereotact Funct Neurosurg* 1996;66:142–5.
15. Chang SD, Adler JR, Jr,, Martin DP. LINAC radiosurgery for cavernous sinus meningiomas. *Stereotact Funct Neurosurg* 1998;71:43–50.
16. Vermeulen S, Young R, Li F, Meier R, Raisis J, Klein S, et al. A comparison of single fraction radiosurgery tumor control and toxicity in the treatment of basal and nonbasal meningiomas. *Stereotact Funct Neurosurg* 1999;72:60–6.
17. Ma Z, Tang J, Qiu B, Hou Y, Peng Z, Liu Y. [Gamma knife treatment of meningiomas] [Abstract]. *Hunan Yi Ke Da Xue Xue Bao* 1998;23:161–3 (in Chinese).
18. Singh VP, Kansai S, Vaishya S, Julka PK, Mehta VS. Early complications following gamma knife radiosurgery for intracranial meningiomas. *J Neurosurg* 2000;93:57–61.
19. Kobayashi T, Kida Y, Mori Y. Long-term results of stereotactic gamma radiosurgery of meningiomas. *Surg Neurol* 2001;55:325–31.
20. Patil CG, Hoang S, Borchers DJ, III, Sakamoto G, Soltys SG, Gibbs IC, et al. Predictors of peritumoral edema after stereotactic radiosurgery of supratentorial meningiomas. *Neurosurgery* 2008;63:435–40; discussion 440–2.
21. Chang JH, Chang JW, Choi JY, Park YG, Chung SS. Complications after gamma knife radiosurgery for benign meningiomas. *J Neurol Neurosurg Psychiatry* 2003;74:226–30.
22. Ganz JC, Schrottner O, Pendl G. Radiation-induced edema after Gamma Knife treatment for meningiomas. *Stereotact Funct Neurosurg* 1996;66:129–33.
23. Kalapurakal JA, Silverman CL, Akhtar N, Laske DW, Braitman LE, Boyko OB, et al. Intracranial meningiomas: factors that influence the development of cerebral edema after stereotactic radiosurgery and radiation therapy. *Radiology* 1997;204:461–5.
24. Cai R, Barnett GH, Novak E, Chao ST, Suh JH. Principal risk of peritumoral edema after stereotactic radiosurgery for intracranial meningioma is tumor-brain contact interface area. *Neurosurgery* 2010;66:513–22.
25. Kollova A, Liscak R, Novotny J, Jr, Vladyka V, Simonova G, Janouskova L. Gamma Knife surgery for benign meningioma. *J Neurosurg* 2007;107:325–36.
26. Novotny J, Jr,, Kollova A, Liscak R. Prediction of intracranial edema after radiosurgery of meningiomas. *J Neurosurg* 2006;105:120–6.
27. Kan P, Liu JK, Wendland MM, Shrieve D, Jensen RL. Peritumoral edema after stereotactic radiosurgery for intracranial meningiomas and molecular factors that predict its development. *J Neurooncol* 2007;83:33–8.
28. Girvigian MR, Chen JC, Rahimian J, Miller MJ, Tome M. Comparison of early complications for patients with convexity and

parasagittal meningiomas treated with either stereotactic radiosurgery or fractionated stereotactic radiotherapy. *Neurosurgery* 2008;62: A19–27.
29. Shiomi H, Inoue T, Nakamura S, Inoue T, Adler JR, Jr, Bodduluri M. [CyberKnife]. *Igaku Butsuri* 2001;21:11–6 (in Japanese).
30. Selch MT, Ahn E, Laskari A, Lee SP, Agazaryan N, Solberg TD, et al. Stereotactic radiotherapy for treatment of cavernous sinus meningiomas. *Int J Radiat Oncol Biol Phys* 2004;59:101–11.
31. National Cancer Institute. Common terminology criteria for adverse events, Version 4.0. <http://evs.nci.nih.gov/ftp1/CTCAE/CTCAE_4.03_2010-06-14_QuickReference_5x7.pdf>.
32. Chen CH, Shen CC, Sun MH, Ho WL, Huang CF, Kwan PC. Histopathology of radiation necrosis with severe peritumoral edema after gamma knife radiosurgery for parasagittal meningioma. A report of two cases. *Stereotact Funct Neurosurg* 2007;85:292–95.
33. Hashiba T, Hashimoto N, Maruno M, Izumoto S, Suzuki T, Kagawa N, et al. Scoring radiologic characteristics to predict proliferative potential in meningiomas. *Brain Tumor Pathol* 2006;23:49–54.
34. Hashiba T, Hashimoto N, Izumoto S, Suzuki T, Kagawa N, Maruno M, et al. Serial volumetric assessment of the natural history and growth pattern of incidentally discovered meningiomas. *J Neurosurg* 2009;110:675–84.

Int. J. Radiation Oncology Biol. Phys., Vol. 80, No. 2, pp. 469–475, 2011

0360-3016/$–see front matter

ELSEVIER

doi:10.1016/j.ijrobp.2010.02.013

CLINICAL INVESTIGATION **Prostate**

MONOTHERAPEUTIC HIGH-DOSE-RATE BRACHYTHERAPY FOR PROSTATE CANCER: FIVE-YEAR RESULTS OF AN EXTREME HYPOFRACTIONATION REGIMEN WITH 54 GY IN NINE FRACTIONS

YASUO YOSHIOKA, M.D., PH.D.,* KOJI KONISHI, M.D.,* IORI SUMIDA, PH.D.,* YUTAKA TAKAHASHI, PH.D.,* FUMIAKI ISOHASHI, M.D.,* TOSHIYUKI OGATA, PH.D.,* MASAHIKO KOIZUMI, M.D., PH.D.,* HIDEYA YAMAZAKI, M.D., PH.D.,† NORIO NONOMURA, M.D., PH.D.,‡ AKIHIKO OKUYAMA, M.D., PH.D.,‡ AND TAKEHIRO INOUE, M.D., PH.D.*

*Department of Radiation Oncology, Osaka University Graduate School of Medicine, Osaka, Japan; †Department of Radiology, Kyoto Prefectural University of Medicine, Kyoto, Japan; ‡Department of Urology, Osaka University Graduate School of Medicine, Osaka, Japan

Purpose: To evaluate an extreme hypofractionation regimen with 54 Gy in nine fractions provided by high-dose-rate (HDR) brachytherapy as monotherapy for prostate cancer by reporting 5-year clinical results.
Methods and Materials: Between 1996 and 2005, 112 patients with localized prostate cancer were treated with HDR brachytherapy without external beam radiotherapy. Of the 112 patients, 15 were considered low risk, 29 intermediate risk, and 68 as high risk. The prescribed dose was uniformly 54 Gy in nine fractions within 5 days. Of the 112 patients, 94 also received hormonal therapy. The median follow-up time was 5.4 years.
Results: All the patients safely completed the treatment regimen. The 5-year prostate-specific antigen (PSA) failure-free, local control, disease-free survival, and overall survival rate was 83%, 97%, 87%, and 96%, respectively. The 5-year PSA failure-free rate for low-, intermediate-, and high-risk patients was 85% (95% confidence interval, 66–100%), 93% (95% confidence interval, 83–100%), and 79% (95% confidence interval, 69–89%), respectively. The significant prognostic factors for PSA failure were the initial PSA level ($p = .029$) and younger age ($p = .019$). The maximal toxicities observed were Grade 3 using the Common Terminology Criteria for Adverse Events, version 3.0, for both acute and late toxicity (6 and 3 patients had acute and late Grade 3 toxicity, respectively). Late Grade 2 toxicity was observed in 13 patients.
Conclusion: Monotherapeutic HDR brachytherapy with an extreme hypofractionation regimen of 54 Gy in nine fractions associated with hormonal therapy was feasible, and its toxicity was acceptable. The interim tumor control rate at a median 5.4 years was promising, even for patients with locally advanced disease. This dose-fractionation scheme might be referred to by other terms, such as stereotactic body radiotherapy. Studies with longer follow-up periods and from multiple institutions are needed to confirm the efficacy of this novel approach. © 2011 Elsevier Inc.

Prostate cancer, Radiotherapy, High-dose-rate brachytherapy, HDR, Monotherapy, Hypofractionation.

INTRODUCTION

Low-dose-rate permanent brachytherapy has become a standard treatment option for early-stage prostate cancer. In contrast, for locally advanced cases, the debate on the role of such brachytherapy regimens is ongoing. As yet, no evidence has confirmed that combining external beam radiotherapy (EBRT) and low-dose-rate brachytherapy improves the outcome (1, 2). Determining the optimal radiotherapy (RT) method, especially for locally advanced prostate cancer, is of the utmost importance.

High-dose-rate (HDR) brachytherapy is in the clinical trial phase and is expected to be able to treat even extracapsular invasive prostate cancer with a more computerized and precise dose distribution. Many investigations (3–9) of HDR brachytherapy have been published since the 1990s; however, all these studies used HDR brachytherapy combined with EBRT. In 2000, however, we (10) were the first to report on the use of HDR brachytherapy without EBRT based on the concept that HDR alone is the most efficient method to escalate the radiation dose to the prostate. In our subsequent reports (11, 12), a promising preliminary outcome and a low rate of acute and late toxicity were reported. Only a few other groups have initiated the use of HDR brachytherapy without EBRT (13–15).

Reprint request to: Yasuo Yoshioka, M.D., Ph.D., Department of Radiation Oncology, Osaka University Graduate School of Medicine, 2-2 (D10) Yamadaoka, Suita, Osaka 565-0871 Japan. Tel: (+81) 6-6879-3482; Fax: (+81) 6-6879-3489; E-mail: yoshioka@radonc.med.osaka-u.ac.jp

Supported in part by a Grant-in-Aid for Young Scientists (B) from Japan Society for the Promotion of Science.
Conflict of interest: none.
Received Nov 3, 2009, and in revised form Jan 9, 2010. Accepted for publication Feb 12, 2010.

The present report is an update on the use of this protocol applied to 112 consecutive patients with a median follow-up period of 5.4 years. In addition, the presented dose-fractionation regimen might be referred to as a model case for extreme hypofractionation in prostate cancer RT.

METHODS AND MATERIALS

Patient characteristics and selection

In January 1994, we launched HDR brachytherapy for prostate cancer at Osaka University Hospital (Osaka, Japan), at first combined with EBRT. In May 1995, we initiated HDR brachytherapy as monotherapy (*i.e.*, without EBRT), which had been, to the best of our knowledge, the first trial in the world of HDR monotherapy (10). The first regimen was 48 Gy in eight fractions within 5 days. In November 1996, we escalated the radiation dose and changed the regimen to 54 Gy in nine fractions within 5 days. From November 1996 through November 2005, 112 consecutive patients were treated with this 54-Gy regimen and were the subjects of the present report. This 54-Gy regimen was closed at that time; and a new regimen with 45.5 Gy in seven fractions within 4 days is now ongoing.

The eligibility criteria were (1) clinical TNM Stage T1c-T3b or T4 with only bladder neck invasion and without nodal or other distant metastases as established by clinical, biochemical, and imaging studies, including magnetic resonance imaging, computed tomography, and bone scans; (2) candidacy for epidural anesthesia; (3) pretreatment transrectal ultrasound (TRUS) and serum prostate-specific antigen (PSA) levels available; and (4) informed consent. Patients were considered ineligible for various reasons, including previous pelvic RT for another malignancy; previous surgery or transurethral resection of the prostate, and prostate cancer recurrence.

The median age at diagnosis was 68 years (range, 47–81). All patients had biopsy-proven adenocarcinoma of the prostate. Using the 2002 International Union Against Cancer TNM staging system, 28 patients had Stage T1, 34 had T2, 46 had T3, and 4 had Stage T4. The initial PSA (iPSA) level was 3.8–233.0 ng/mL (median, 16.6), including 31 patients with a PSA level <10.0 ng/mL, 31 with 10.0–19.9 ng/mL, and 50 with a PSA level of ≥20.0 ng/mL. Of the 112 patients, 50 had a Gleason score of ≤6, 36 had Gleason score 7, and 26 had Gleason score of ≥8. We defined low-risk patients as those with an iPSA <10.0 ng/mL, Gleason score of ≤6, and Stage T1c-T2a; intermediate-risk patients as those with an iPSA level of ≥10 but <20 ng/mL, Gleason score 7, or Stage T2b-T2c; and high-risk patients as those with an iPSA level of ≥20.0 ng/mL, Gleason score of ≥8, or Stage T3-T4. Of the 112 patients, 15 were classified as low risk, 29 as intermediate risk, and 68 as high risk (Table 1).

Table 1. Patient characteristics

Characteristic	Value
Patients (*n*)	112
Age	
Median	68
Range	47–81
T classification	
T1	28
T2	34
T3	46
T4	4
Gleason score	
2–4	15
5–6	35
7	36
8–10	26
Pretreatment PSA (ng/mL)	
<10.0	31
10.0–20.0	31
≥20.0	50
Median	16.6
Range	3.8–233.0
Risk group*	
Low	15
Intermediate	29
High	68
Hormonal therapy	
Yes	94
No	18
Follow-up (y)	
Median	5.4
Range	1.3–11.4

Abbreviation: PSA = prostate-specific antigen.

* Low, T1c-T2a, Gleason score ≤6, and PSA <10 ng/mL; intermediate, T2b-T2c, Gleason score 7, or PSA ≥10 but <20 ng/mL; and high, T3-T4, Gleason score ≥8, or PSA ≥20 ng/mL.

Hormonal therapy

The treatment protocol for hormonal therapy was as follows. Patients with a large prostate volume (>40 cm^3), those with intermediate- or high-risk cancer underwent 6–12 months of neoadjuvant hormonal therapy, and high-risk patients underwent 3 years or lifetime adjuvant hormonal therapy. Both neoadjuvant and adjuvant hormonal therapy included luteinizing hormone-releasing hormone agonists and antiandrogens. The final decisions concerning hormonal therapy were made by the urologists.

Of the 112 patients, 18 (16%) received no hormonal therapy and 94 (84%) underwent neoadjuvant and/or adjuvant hormonal therapy, with a median duration of 36 months (range, 2–131). Of these 94 patients, 59 (53%) had finished their hormonal therapy by the last follow-up, with a median duration of hormonal therapy of 22 months (range, 2–120), and 35 (31%) were still receiving hormonal therapy at their last follow-up visit, with a median duration of 71 months (range, 20–131). Of the 15 low-risk patients, 6 received no hormonal therapy, 8 had finished neoadjuvant and/or adjuvant hormonal therapy, with a median duration of 14 months (range, 5–36), and 1 had been receiving hormonal therapy for 25 months at their last follow-up visit. Of the 29 intermediate-risk patients, 10 received no hormonal therapy, 17 had finished hormonal therapy, with a median duration of 11 months (range, 3–53), and 2 had been receiving hormonal therapy for 74 and 98 months at their last follow-up visit. Of the 68 high-risk patients, 2 received no hormonal therapy, 34 had finished hormonal therapy, with a median duration of 29 months (range, 2–120), and 32 had been receiving hormonal therapy for a median duration of 71 months (range, 20–131).

Implant technique

The implant technique has been previously described in detail by us (10). In brief, it involved continuous epidural anesthesia, real-time TRUS guidance, the use of metallic applicators and applicator stoppers (Trocar Point Needles and Needle Stoppers, Nucletron, Veenendaal, The Netherlands), and an original template and its cover plate (Taisei Medical, Osaka, Japan).

Under real-time TRUS monitoring of the largest cross-section of the prostate, the applicators were placed on the line encompassing the prostate (with or without extracapsular invasion) and within

the prostate, but sparing the urethra, at 1–1.5-cm intervals. For the posterior (rectal) side, the applicators were placed 0–3 mm inside the prostatic capsule. The top 2 cm of the catheters were placed within the bladder pouch. When a seminal vesicle was included in the target, the placement of some applicators involved piercing the medial one-half of the seminal vesicle.

Treatment planning and RT

The clinical target volume (CTV) included the whole prostate gland plus 5 mm in all directions, except for the posterior (rectal) margin. The posterior margin varied from 2 to 5 mm, depending on the distance to the rectal wall. If extracapsular invasion was observed or strongly suspected, that area with a 5-mm margin was included in the CTV. If seminal vesicle invasion was observed or strongly suspected, the medial one-half of the seminal vesicle with a 5-mm margin was also included in the CTV. The planning target volume (PTV) was equal to the CTV, except for in the cranial direction, where it was larger. The top 2 cm of the applicators were placed within the bladder pouch, such that the PTV included a 1-cm margin in the cranial direction from the CTV. This margin was established, not only to avoid the cold area at the base of the prostate, but also to compensate for possible needle displacement in the caudal direction. At 1 hour before each radiation fraction, a urinary balloon catheter was clipped in place to keep the urine within the bladder pouch so that the opposite side of the bladder wall and bowel were kept away from the radiation field.

Treatment planning was done with the aid of PLATO (Nucletron) using geometric optimization (volume method) and one prescription dose point. The prescription dose point was positioned 5 mm distant from one source in the central plane. In principle, that source was the closest one to the rectum, and the prescription dose point was in the direction of the rectum (*i.e.*, outside the prostate). The source dwell positions were located on the prostate surface and inside the prostate (except for in the cranial direction, where it was located 1 cm outside the prostate). The dose constraints were as follows: the dose to the whole urethra should be 100–150% of the prescription dose, and the dose to the whole rectal mucosa should be <100% of the prescription dose. According to our previous analyses (10, 11), a volume receiving ≥100% of the prescription dose, regardless of the PTV, of <60 cm^3 and a dose nonuniformity ratio (volume receiving ≥150% of the prescription dose/volume receiving ≥100% of the prescription dose) of <30% were preferred, but they were not adopted as constraints.

The patients remained in bed with epidural anesthesia for 5 days from Monday to Friday and underwent RT twice daily, with an interval of ≥6 h. The treatment consisted of nine fractions of 6.0 Gy each (total 54 Gy). The isoeffective dose used in the present study corresponded to approximately 116 Gy administered at 2 Gy/fraction, according to the linear-quadratic model and with the assumption of an α/β ratio of 1.5 Gy for prostate cancer or 97 Gy with the assumption of an α/β ratio of 3 Gy (16, 17). Prophylactic antibiotics were administered twice daily from the day of implant through Day 7. Air pumping devices were attached to the patients' lower legs to prevent deep vein thrombosis from the day of implant through Day 5.

To ensure the correct needle position, radiation oncologists confirmed that no abnormal space was present between the perineum and template, no unexpected edema was present in the perineum, and none of the needle ends protruded unexpectedly compared with the others before each RT session. However, we did not perform routine repositioning of the inserted needles before each session (*e.g.*, radiography before each RT session). We used a 1-cm PTV margin in the cranial direction so that it covered the CTV adequately even when the needles had moved in the caudal direction ≤1 cm. We had collected data on needle displacement in the very early period of the present study and had found that unexpected changes in needle position were distributed between 0 and 1 cm in the caudal direction in most sessions for most patients. However, the data were not meant for publication. We are planning to reassess needle displacement but have not yet done so.

Follow-up and toxicity analysis

A radiation oncologist and urologist performed the follow-up evaluations, including PSA determinations and queries about urinary and bowel symptoms, at least every 3 months. Magnetic resonance imaging was performed at least every 2 years during the follow-up period for all patients. PSA failure was defined as the nadir plus 2 ng/mL according to the Radiation Therapy Oncology Group/American Society for Therapeutic Radiology and Oncology Phoenix Consensus Conference recommendations (18). The PSA level was examined using AIA-PACK PA (Tosoh, Tokyo, Japan). Acute and late toxicity was scored according to the Common Terminology Criteria for Adverse Events, version 3.0 (19). Acute toxicity was defined as symptoms observed during or after treatment that had completely resolved by 6 months after treatment. Treatment-related toxicity that persisted >6 months after treatment completion were considered late toxicity. The toxicity data were collected retrospectively by chart review. During the study period, we did not use any prospective patient-administered quality-of-life instruments. The median follow-up for the present study was 5.4 years (range, 1.3–11.4).

Statistical analysis

Local control, overall survival, disease-free survival, and PSA failure-free rates were calculated using the Kaplan-Meier method (20). Univariate and multivariate analysis was performed for PSA failure using a Cox proportional hazards model. p Values <.05 were considered significant.

RESULTS

Feasibility

All 112 patients completed the treatment regimen. No significant intraoperative or perioperative complications requiring treatment modification occurred.

Clinical outcome

Of the 112 patients, 19 developed PSA failure, with 14 showing evidence of clinical events, including 3 with local recurrence only, 1 with lymph node metastases only, 8 with bone metastases only, 1 with both bone and lymph node metastases, and 1 with bone and lymph node metastases and local recurrence. Of the 112 patients, 4 died of prostate cancer and 1 of intercurrent disease. All 5 patients had belonged to the high-risk group.

The 5-year local control, overall survival, disease-free survival, and PSA failure-free rate was 97%, 96%, 87%, and 83%, respectively (Fig. 1). The 5-year PSA failure-free rate for the low-, intermediate-, and high-risk groups was 85% (95% confidence interval, 66–100%), 93% (95% confidence interval, 83–100%), and 79% (95% confidence interval, 69–89%), respectively (Fig. 2).

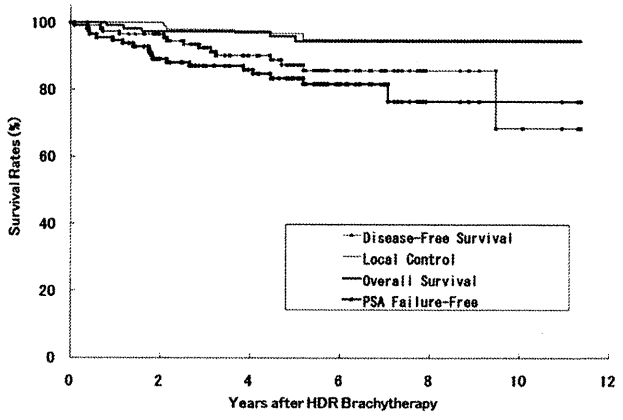

Fig. 1. Local control, overall survival, disease-free survival, and PSA failure-free rates for all 112 patients.

Univariate and multivariate analysis revealed that iPSA ($p = .029$) and younger age ($p = .019$) were significant prognostic factors for PSA failure. A Gleason score of ≥7 had a tendency toward a greater PSA failure rate ($p = .123$; Table 2).

Table 2. Univariate and multivariate analysis for PSA failure using Cox proportional hazards model

	Univariate analysis		Multivariate analysis	
Variable	HR (95% CI)	*p*	HR (95% CI)	*p*
Age	0.930 (0.869–0.995)	.035	0.920 (0.857–0.986)	.019
PSA	1.010 (1.003–1.017)	.009	1.010 (1.001–1.019)	.029
Gleason score		.050		.123
≤6	1.000 (Referent)		1.000 (Referent)	
≥7	3.014 (0.999–9.091)		2.314 (0.797–6.714)	
T classification		.227		.619
T1–T2	1.000 (Referent)		1.000 (Referent)	
T3–T4	1.754 (0.705–4.367)		0.739 (0.224–2.439)	
Risk group		.098		.460
Low-intermediate	1.000 (Referent)		1.000 (Referent)	
High	2.536 (0.841–7.646)		1.716 (0.409–7.197)	

Abbreviations: HR = hazard ratio; CI = confidence interval; PSA = prostate-specific antigen.

Acute toxicity

No Grade 4 or 5 acute toxicity was detected. However, 6 patients (5%) had Grade 3 acute toxicity (3 with urinary frequency/urgency and 1 each with hematuria, retention, and urinary pain). Grade 2 acute toxicity developed in 21 patients (19%), all of whom recovered without special treatment, and 58 patients (52%) developed Grade 1 acute toxicity only. The details of acute toxicity that occurred with this treatment approach are listed in Table 3. A total of 4 patients (4%) required urethral catheterization in the acute phase because of Grade 3 or Grade 2 retention (Table 3). Temporary events, such as hematuria during or just after implantation or detachment of the needles, were not considered acute radiation toxicity, because such events were caused by mechanical stimulation of the needles, and the patients recovered without treatment within a few hours.

Late toxicity

No Grade 4 or 5 late toxicity was detected. Grade 3 late toxicity developed in 3 patients (3%), 1 of whom developed a sigmoid colon perforation 7 years after HDR brachytherapy and underwent surgical treatment, including colostomy. No clear relationship between HDR brachytherapy to the prostate and the sigmoid colon perforation could be established. Another patient developed a rectourethral fistula 4 years after HDR brachytherapy. He had undergone a laser coagulation procedure against rectal bleeding. Another patient developed severe urethral stenosis and underwent surgery 4 years after HDR brachytherapy.

A total of 13 patients (12%) developed Grade 2 late toxicity, including 6 cases of rectal bleeding, 2 of urinary frequency/urgency, 2 of urinary pain, and 1 each of hematuria,

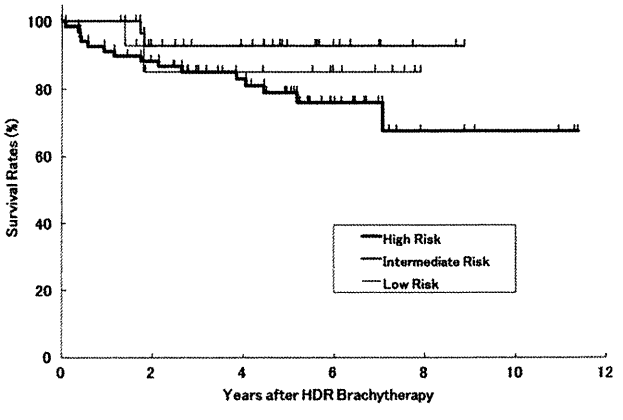

Fig. 2. PSA failure-free rates for patients stratified by the risk group.

Table 3. Acute toxicities

Grade	Adverse event	Patients (*n*)
5		0
4		0
3		
	Urinary frequency/urgency	3
	Genitourinary hemorrhage (bladder or urethra)	1
	Urethral pain	1
	Urinary retention	1
2		
	Urinary frequency/urgency	13
	Genitourinary hemorrhage (bladder or urethra)	3
	Urinary retention	3
	Constipation	1
	Anal pain	1
1		58
0		27

Grade determined using Common Terminology Criteria for Adverse Events, version 3.0.

dysuria, and retention. Finally, 26 (23%) developed Grade 1 late toxicity only (Table 4).

DISCUSSION

Radiation dose escalation with high conformity has been an essential component of attempts to achieve better treatment results with RT for localized prostate cancer (21). HDR brachytherapy is one of the most efficient modalities for that purpose because of its excellent conformity and rapid dose falloff outside the target volume. Historically, HDR brachytherapy has been performed as a boost after EBRT (3–9, 22–24). However, this combination method typically takes an additional 4–5 weeks for EBRT, in addition to hospitalization for HDR brachytherapy. In contrast, if a satisfactory dose distribution could be achieved with HDR brachytherapy alone, without EBRT, it would definitely be the most efficient method to achieve high conformity and dose escalation. Thus, we initiated HDR brachytherapy without EBRT; to the best of our knowledge, the first such treatment reported in published studies (10). Some other groups subsequently initiated HDR brachytherapy without EBRT (13–15) (Table 5).

High-dose-rate brachytherapy has many advantages in terms of radiation physics, including good tumor coverage, even for extracapsular tissue, homogeneous dose distribution, no radiation exposure to the medical staff, and no need to isolate patients in highly shielded rooms. Some investigators have suggested that HDR brachytherapy is superior to conformal EBRT or low-dose-rate permanent brachytherapy in terms of dosimetry (25, 26). The developments in remote afterloading brachytherapy devices and computer algorithms have made anatomy-related dose optimization possible (*i.e.*, adaptation of dwell locations and dwell times of the stepping source to the target and no impairment from edema, source migration, or prostate movement during the short treatment course) and significantly lowered the costs of remote afterloading treatment (27, 28).

Table 4. Late toxicities

Grade	Adverse event	Patients (*n*)
5		0
4		0
3		
	Rectourethral fistula	1
	Gastrointestinal perforation of sigmoid colon	1*
	Urethral stricture/stenosis	1
2	Grade	
	Rectal hemorrhage	6
	Urinary frequency/urgency	2
	Urethral pain	2
	Genitourinary hemorrhage (bladder or urethra)	1
	Urethral stricture/stenosis	1
	Urinary retention	1
1		26
0		70

Grade determined using Common Terminology Criteria for Adverse Events, version 3.0.

* Relationship between perforation and high-dose-rate brachytherapy was unclear.

The method we used to determine our dose fractionation schedule (54 Gy in nine fractions) has been previously reported (12). From the viewpoint of radiation biology, prostate cancer might have a very low α/β ratio of about 1.5 Gy (17). Thus, a radiation dose fractionation regimen with a high dose/fraction such as ours (6 Gy/fraction) has advantages compared with a conventional dose/fraction (*e.g.*, 2 or 1.8 Gy/fraction for EBRT) or permanent brachytherapy. In addition, a regimen of HDR brachytherapy alone could be expected to maximize this advantage compared with a combination regimen of HDR brachytherapy and EBRT. The isoeffective dose used in the present study corresponded to approximately 116 Gy administered at 2 Gy/fraction using the linear-quadratic model and assuming an α/β ratio of 1.5 Gy for prostate cancer or 97 Gy, assuming an α/β ratio of 3 Gy (16, 17). This isoeffective dose was significantly greater than that used with other RT modalities. For example, a well-known technique for dose escalation is intensity-modulated RT, used at the Memorial Sloan-Kettering Cancer Center, with 81.0 Gy or 86.4 Gy delivered (29).

Hypofractionation is one of the greatest concerns in the field of EBRT for prostate cancer. Several randomized and nonrandomized trials have indicated the noninferiority of hypofractionated regimens (30–32). The typical up-to-date technique with a linear accelerator might be image-guided intensity-modulated RT, in which the dose/fraction is usually 2.5–3.0 Gy. However, very recently, the enthusiasm for extreme hypofractionated regimens has been driven by several forces, including patient convenience, developing technologies, and preclinical data suggesting fewer, larger fractions might increase the therapeutic ratio in prostate cancer (33). However, the available clinical data are very few. The typical technology used for extreme hypofractionated regimens has included HDR monotherapy and stereotactic body RT. No consensus exists on the dosage, fractionation, technique, or normal tissue constraints. For example, a HDR monotherapy regimen other than ours delivered 31.5–38 Gy in three to four fractions of 8.5–10.5 Gy (13–15), and a stereotactic regimen delivered 33.5–36.25 Gy in five fractions of 6.7–7.25 Gy (34, 35). If such a consensus evolves, it might enable extreme hypofractionated regimens to be compared with conventionally fractionated approaches, although no direct comparisons (randomized controlled trials) of extreme hypofractionation have been planned.

The clinical results obtained with our protocol have been encouraging. The 5-year PSA failure-free rate for low-, intermediate-, and high-risk groups was 85%, 93%, and 79%, respectively; comparable to previously reported results. This can be attributed to the very high isoeffective dose administered, which might have been an adequate dose to control even the locally advanced cases in the present study.

Regarding toxicity, the monotherapeutic HDR brachytherapy protocol also proved promising. Although we administered a very high isoeffective dose, only 3 patients developed Grade 3 late toxicity. All other patients with Grade

Table 5. Regimen and outcome of HDR brachytherapy with or without EBRT

Investigator	Start year	Patients (*n*)	HDR brachytherapy	EBRT	Risk group	5-y PSA failure-free rate (%)	Grade 2 or more late toxicity rate (%)
Galalae *et al.* (3)	1986	144	30 Gy/2 Fr	40 Gy/20 Fr	Low to high	74	11*
Borghede *et al.* (4), Aström *et al.* (22)	1988	214	20 Gy/2 Fr	50 Gy/25 Fr	Low to high	82	17*
Mate *et al.* (5)	1989	104	12–16 Gy/4 Fr	50.4 Gy/28 Fr	Low to high	84	12
Demanes *et al.* (6)	1991	209	24 Gy/4 Fr	36 Gy/20 Fr	Low	90	18
					Intermediate	87	
					High	69	
Martinez *et al.* (7), Vargas *et al.* (23)	1991	197	16.5–19.5 Gy/3 Fr, 16.5–23 Gy/2 Fr	46 Gy/23 Fr	Intermediate to high	81	15*
Dinges *et al.* (8), Deger *et al.* (24)	1992	442	18–20 Gy/2 Fr	40 Gy/20 Fr, 45 Gy/25 Fr, 50.4 Gy/28 Fr	Low to high	65	11†
Hiratsuka *et al.* (9)	1997	71	16.5 Gy/3 Fr, 22 Gy/4 Fr	45 Gy/25 Fr, 41.8 Gy/19 Fr	Low to high	93	10
Martinez *et al.* (13)	1999	41	38 Gy/4 Fr	–	Low	–	–
Martin *et al.* (14)	2002	82	38 Gy/4 Fr	–	Low	–	–
Corner *et al.* (15)	2003	110	34 Gy/4 Fr, 36 Gy/4 Fr, 31.5 Gy/3 Fr	–	Low to high	–	–
Present study	1996	112	54 Gy/9 Fr	–	Low	85	14
					Intermediate	93	
					High	79	

Abbreviations: HDR = high-dose-rate; EBRT = external beam radiotherapy; Fr = fractions.
* Data for gastrointestinal toxicity alone.
† Data for Grades 3 and 4.

1 or 2 toxicity recovered without any special treatment, except for medication. The low rate of late toxicity seen in our study might be attributable to the highly conformal dose distribution of HDR brachytherapy and the small radiation volume. The steep dose falloff reduced the radiation exposure to the adjacent normal tissues (*i.e.*, rectum and bladder), and the dose optimization process spared the dose of the organ at risk inside the prostate (*i.e.*, urethra). We have previously demonstrated that the smaller irradiated volume was related to the lower rate of acute and late toxicity (11, 36) and that the more sophisticated algorithm used by the planning computer could reduce the dose to the urethra more efficiently while maintaining the dose to the prostate (28). However, underreporting and underestimating the toxicity was possible owing to the retrospective nature of data collection in the present study.

One of the major limitations of the present study was the high rate of use of hormonal therapy. Its duration varied widely and, in some cases, was substantially long. This might have been a result of the characteristics of Japanese clinical practice, because, in some reports (37), 95% of the EBRT patients with localized prostate cancer received hormonal therapy. The main reason was probably that no limit has been placed on the reimbursement by the Japanese health insurance system for the cost of hormonal therapy once the patient has been diagnosed with prostate cancer, regardless of the type of accompanying therapy. Moreover, medical insurance in Japan is a system of universal health coverage. This mix of hormonal therapy might have compromised the results of HDR brachytherapy. Another limitation was that, for prostate cancer, the median follow-up (5.4 years) was still too short for any definitive conclusions with regard to tumor control. Moreover, this was a single-institution experience.

Finally, the findings from the present report indicate that monotherapeutic HDR brachytherapy with an extreme hypofractionation regimen of 54 Gy in nine fractions combined with hormonal therapy was feasible and its toxicity acceptable. The interim tumor control rate at a median of 5.4 years was promising, even for locally advanced cases. However, reports with longer follow-up periods and from multiple institutions are needed to confirm the efficacy of this novel approach.

REFERENCES

1. Nag S, Beyer D, Friedland J, *et al.* American Brachytherapy Society (ABS) recommendations for transperineal permanent brachytherapy of prostate cancer. *Int J Radiat Oncol Biol Phys* 1999;44:789–799.
2. Ash D, Flynn A, Battermann J, *et al.* ESTRO/EAU/EORTC recommendations on permanent seed implantation for localized prostate cancer. *Radiother Oncol* 2000;57:315–321.
3. Galalae RM, Kovacs G, Schultze J, *et al.* Long-term outcome after elective irradiation of the pelvic lymphatics and local dose escalation using high-dose-rate brachytherapy for locally advanced prostate cancer. *Int J Radiat Oncol Biol Phys* 2002; 52:81–90.
4. Borghede G, Hedelin H, Holmang S, *et al.* Combined treatment with temporary short-term high dose rate iridium-192

brachytherapy and external beam radiotherapy for irradiation of localized prostatic carcinoma. *Radiother Oncol* 1997;44:237–244.
5. Mate TP, Gottesman JE, Hatton J, *et al.* High dose-rate afterloading Ir-192 prostate brachytherapy: Feasibility report. *Int J Radiat Oncol Biol Phys* 1998;41:525–533.
6. Demanes DJ, Rodriguez RR, Schour L, *et al.* High-dose-rate intensity-modulated brachytherapy with external beam radiotherapy for prostate cancer: California endocurietherapy's 10-year results. *Int J Radiat Oncol Biol Phys* 2005;61:1306–1316.
7. Martinez A, Gonzalez J, Stromberg J, *et al.* Conformal prostate brachytherapy: Initial experience of a phase I/II dose escalating trial. *Int J Radiat Oncol Biol Phys* 1995;33:1019–1027.
8. Dinges S, Deger S, Koswig S, *et al.* High-dose rate interstitial with external beam irradiation for localized prostate cancer—Results of a prospective trial. *Radiother Oncol* 1998;48:197–202.
9. Hiratsuka J, Jo Y, Yoshida K, *et al.* Clinical results of combined treatment conformal high-dose-rate iridium-192 brachytherapy and external beam radiotherapy using staging lymphadenectomy for localized prostate cancer. *Int J Radiat Oncol Biol Phys* 2004;59:684–690.
10. Yoshioka Y, Nose T, Yoshida K, *et al.* High-dose-rate interstitial brachytherapy as a monotherapy for localized prostate cancer: Treatment description and preliminary results of a phase I/II clinical trial. *Int J Radiat Oncol Biol Phys* 2000;48:675–681.
11. Yoshioka Y, Nose T, Yoshida K, *et al.* High-dose-rate brachytherapy as monotherapy for localized prostate cancer: A retrospective analysis with special focus on tolerance and chronic toxicity. *Int J Radiat Oncol Biol Phys* 2003;56:213–220.
12. Yoshioka Y, Konishi K, Oh RJ, *et al.* High-dose-rate brachytherapy without external beam irradiation for locally advanced prostate cancer. *Radiother Oncol* 2006;80:62–68.
13. Martinez A, Pataki I, Edmundson G, *et al.* Phase II prospective study of the use of conformal high-dose-rate brachytherapy as monotherapy for the treatment of favorable stage prostate cancer: A feasibility report. *Int J Radiat Oncol Biol Phys* 2001; 49:61–69.
14. Martin T, Baltas D, Kurek R, *et al.* 3-D conformal HDR brachytherapy as monotherapy for localized prostate cancer: A pilot study. *Strahlenther Onkol* 2004;180:225–232.
15. Corner C, Rojas AM, Bryant L, *et al.* A Phase II study of high-dose-rate afterloading brachytherapy as monotherapy for the treatment of localized prostate cancer. *Int J Radiat Oncol Biol Phys* 2008;72:441–446.
16. Fowler JF. The linear-quadratic formula and progress in fractionated radiotherapy. *Br J Radiol* 1989;62:679–694.
17. Brenner DJ, Hall EJ. Fractionation and protraction for radiotherapy of prostate carcinoma. *Int J Radiat Oncol Biol Phys* 1999; 43:1095–1101.
18. Roach M III, Hanks G, Thames H Jr., *et al.* Defining biochemical failure following radiotherapy with or without hormonal therapy in men with clinically localized prostate cancer: Recommendations of the RTOG-ASTRO Phoenix Consensus Conference. *Int J Radiat Oncol Biol Phys* 2006; 65:965–974.
19. National Cancer Institute. Common Terminology Criteria for Adverse Events, version 3.0. Available from: www.ctep.info.nih.gov/protocolDevelopment/electronic_applications/docs/ctcaev3.pdf. Accessed October 9, 2009.
20. Kaplan EL, Meier P. Nonparametric estimation from incomplete observation. *J Am Stat Assoc* 1958;53:457–481.
21. Pollack A, Zagars GK, Smith LG, *et al.* Preliminary results of a randomized radiotherapy dose-escalation study comparing 70 Gy with 78 Gy for prostate cancer. *J Clin Oncol* 2000;18: 3904–3911.
22. Aström L, Pedersen D, Mercke C, *et al.* Long-term outcome of high dose rate brachytherapy in radiotherapy of localised prostate cancer. *Radiother Oncol* 2005;74:157–161.
23. Vargas CE, Martinez AA, Boike TP, *et al.* High-dose irradiation for prostate cancer via a high-dose-rate brachytherapy boost: Results of a phase I to II study. *Int J Radiat Oncol Biol Phys* 2006;66:416–423.
24. Deger S, Boehmer D, Roigas J, *et al.* High dose rate (HDR) brachytherapy with conformal radiation therapy for localized prostate cancer. *Eur Urol* 2005;47:441–448.
25. Hsu IC, Pickett B, Shinohara K, *et al.* Normal tissue dosimetric comparison between HDR prostate implant boost and conformal external beam radiotherapy boost: Potential for dose escalation. *Int J Radiat Oncol Biol Phys* 2000;46:851–858.
26. Wang Y, Sankreacha R, Al-Hebshi A, *et al.* Comparative study of dosimetry between high-dose-rate and permanent prostate implant brachytherapies in patients with prostate adenocarcinoma. *Brachytherapy* 2006;5:251–255.
27. Kovacs G, Potter R, Loch T, *et al.* GEC/ESTRO-EAU recommendations on temporary brachytherapy using stepping sources for localised prostate cancer. *Radiother Oncol* 2005;74:137–148.
28. Yoshioka Y, Nishimura T, Kamata M, *et al.* Evaluation of anatomy-based dwell position and inverse optimization in high-dose-rate brachytherapy of prostate cancer: A dosimetric comparison to a conventional cylindrical dwell position, geometric optimization, and dose-point optimization. *Radiother Oncol* 2005;75:311–317.
29. Zelefsky MJ, Fuks Z, Hunt M, *et al.* High-dose intensity modulated radiation therapy for prostate cancer: Early toxicity and biochemical outcome in 772 patients. *Int J Radiat Oncol Biol Phys* 2002;53:1111–1116.
30. Lukka H, Hayter C, Julian JA, *et al.* Randomized trial comparing two fractionation schedules for patients with localized prostate cancer. *J Clin Oncol* 2005;23:6132–6138.
31. Yeoh EE, Holloway RH, Fraser RJ, *et al.* Hypofractionated versus conventionally fractionated radiation therapy for prostate carcinoma: Updated results of a phase III randomized trial. *Int J Radiat Oncol Biol Phys* 2006;66:1072–1083.
32. Kupelian PA, Willoughby TR, Reddy CA, *et al.* Hypofractionated intensity-modulated radiotherapy (70 Gy at 2.5 Gy per fraction) for localized prostate cancer: Cleveland Clinic experience. *Int J Radiat Oncol Biol Phys* 2007;68:1424–1430.
33. Lee WR. Extreme hypofractionation for prostate cancer. *Expert Rev Anticancer Ther* 2009;9:61–65.
34. Madsen BL, Hsi RA, Pham HT, *et al.* Stereotactic hypofractionated accurate radiotherapy of the prostate (SHARP), 33.5 Gy in five fractions for localized disease: First clinical trial results. *Int J Radiat Oncol Biol Phys* 2007;67:1099–1105.
35. King CR, Brooks JD, Gill H, *et al.* Stereotactic body radiotherapy for localized prostate cancer: Interim results of a prospective phase II clinical trial. *Int J Radiat Oncol Biol Phys* 2009;73: 1043–1048.
36. Konishi K, Yoshioka Y, Isohashi F, *et al.* Correlation between dosimetric parameters and late rectal and urinary toxicities in patients treated with high-dose-rate brachytherapy used as monotherapy for prostate cancer. *Int J Radiat Oncol Biol Phys* 2009;75:1003–1007.
37. Yoshioka Y, Suzuki O, Kobayashi K, *et al.* External-beam radiotherapy for clinically localized prostate cancer in Osaka, Japan, 1995–2006: Time trends, outcome, and risk stratification. *Strahlenther Onkol* 2009;185:446–452.

Radiation Oncology

BioMed Central
The Open Access Publisher

Evaluation of heterogeneity dose distributions for Stereotactic Radiotherapy (SRT) : Comparison of commercially available Monte Carlo dose calculation with other algorithms.

Radiation Oncology 2012, **7**:20 doi:10.1186/1748-717X-7-20

Wataru Takahashi (wataru.harry1@gmail.com) Hideomi Yamashita (yamachan07291973@yahoo.co.jp) Naoya Saotome (as.if.nao@gmail.com)
Yoshio Iwai (Yoshio.Iwai@elekta.com)
Akira Sakumi (sakumiakira18@gmail.com)
Akihiro Haga (haga@rcnp.osaka-u.ac.jp)
Keiichi Nakagawa (k-nak@fg7.so-net.ne.jp)

ISSN 1748-717X

Article type Research

Submission date 12 September 2011

Acceptance date 9 February 2012

Publication date 9 February 2012

Article URL http://www.ro-journal.com/content/7/1/20